



## A Review of the Use of Microwave Radiometry in Space Geodesy



Gunnar Elgered  
Department of Radio and Space Science  
Onsala Space Observatory  
Chalmers University of Technology

presented at the  
Workshop on Measurement of Atmospheric Water Vapour: Theory, Techniques,  
Astronomical and Geodetic Applications, Wettzell / Hoellenstein (Germany),  
October 9–11, 2006



## Presentation Structure

- My interpretation of space geodesy — relevant applications
- Types of microwave radiometers for estimation of the wet delay
- WVR data as corrections in VLBI data analyses
- GPS applications: H<sub>2</sub>O as noise and as a signal
- Characterization of wet path delay variations
- Conclusions: the role of microwave radiometry in support of space geodesy

## Space Geodesy:

### Precise positioning using signal sources in space

- Satellite doppler techniques — radio
- Very-Long-Baseline Interferometry (VLBI) — radio
- Satellite Laser Ranging — optical
- Lunar Laser Ranging (LLR) — optical
- Global Positioning System (GPS) — radio
- Doppler Orbitography and Radiopositioning Integrated by Satellite (DORIS)
- Satellite altimetry (e.g. on TOPEX / Poseidon)

### GPS meteorology?

## Comparison of VLBI, GPS, and DORIS

- VLBI and GPS have passive ground stations whereas DORIS is active.
- All using microwaves and two frequencies for ionospheric corrections.  
GPS: 1.2 / 1.6 GHz, VLBI: 2.3 / 8.4 GHz, DORIS: 0.4 / 2.0 GHz
- All techniques use mapping functions for the elevation dependence.
- VLBI use highly directive antennas and sequential observations towards signal sources, whereas GPS and DORIS use hemispherical antennas and suffer from multipath and signal scattering.
- GPS is superior in terms of spatial (and temporal) sampling — GNSS (including Galileo) even better!
- DORIS has higher short term noise.

### Zenith Delay Estimates from VLBI, GPS, and DORIS

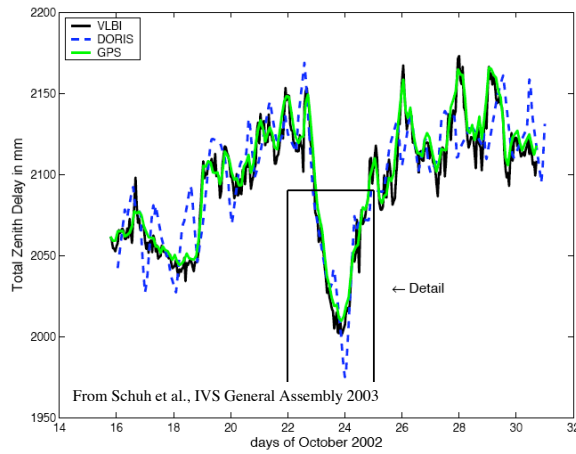
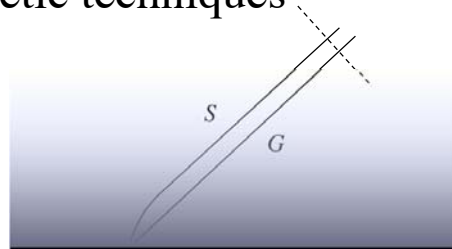


Figure 1. Total zenith delays at Hartebeesthoek during CONT02.

### The effect of the neutral atmosphere on space geodetic techniques

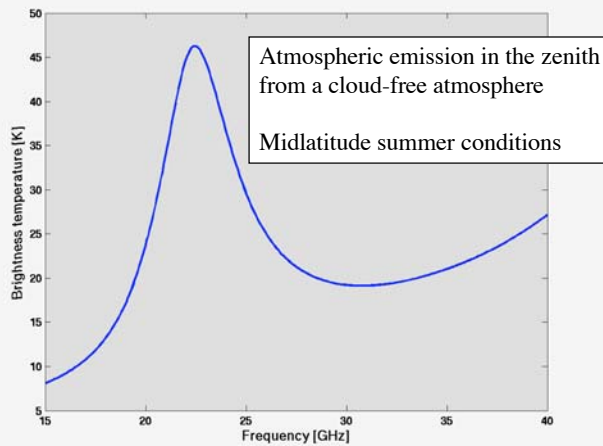


The excess propagation path:

$$\Delta L = \int_S n ds - G = \int_S (n - 1) ds + S - G$$

The radio path length      The straight line distance      The delay due to bending

The water vapour emission line at 22 GHz has about the right strength to make the atmosphere optically thin (for most conditions)



Measurements  
can be used to  
infer integrated  
quantities

### Inferring the wet delay from sky brightness temperatures (1)

$$N = 10^{-6} (n - 1) = k_1 \frac{p_d}{T} Z_d^{-1} + k_2 \frac{e}{T} Z_w^{-1} + k_3 \frac{e}{T^2} Z_w^{-1}$$

$$\Delta L_h = (0.0022768 \pm 0.0000024 \text{ (m/mbar)}) \frac{P_o}{f(\Phi, H)}$$

where

$$f(\Phi, H) = (1 - 0.00266 \cos 2\Phi - 0.00028H)$$

$$\Delta L_w = 10^{-6} \left[ (24 \pm 10) \int_S \frac{e}{T} Z_w^{-1} ds + (3.754 \pm 0.030) \times 10^5 \int_S \frac{e}{T^2} Z_w^{-1} ds \right]$$

The wet delay is an integrated quantity depending on the partial pressure of water vapour and the temperature in the atmosphere

An uplooking microwave radiometer observes the sky brightness temperature:

$$T_{b,f} = T_{bg} e^{-\tau_\infty} + \int_0^\infty T(s) \alpha(f, s) e^{-\tau(f,s)} ds$$

$$\alpha = \alpha_v + \alpha_{ox} + \alpha_\ell$$

The opacity  $\tau(f, s)$  is defined as:

$$\tau(f, s) = \int_0^s \alpha(f, s') ds'$$

The observed sky brightness temperature is an integrated quantity depending on the partial pressure of water vapour, the pressure, the amount of liquid water, and the temperature in the atmosphere

Algorithms for inferring the wet delay from observed sky brightness temperatures

$$T_{b,f} = T_{bg} e^{-\tau_\infty} + T_m(f) (1 - e^{-\tau_\infty})$$

$$\tau_\infty = -\ln \left( \frac{T_m - T_{bg}}{T_m - T_{b,f}} \right)$$

We may also define linearized sky brightness temperature

$$T'_{b,f} = T_{bg} + \int_0^\infty (T(s) - T_{bo,f}) \alpha(f, s) ds$$

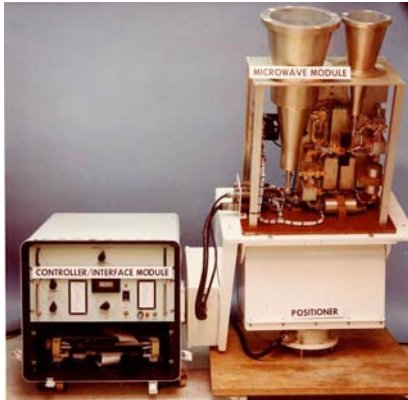
$$\Delta L_w = c_\tau \left[ \left( \frac{f_2}{f_1} \right)^2 \tau_{a,f_1} - \tau_{a,f_2} - \tau_{corr} \right]$$

$$\Delta L_w = c_T \left[ \left( \frac{f_2}{f_1} \right)^2 T'_{a,f_1} - T'_{a,f_2} - T_{corr} \right]$$

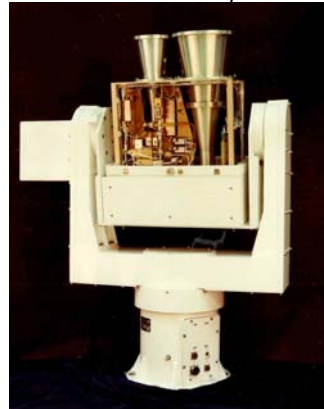
Many studies exist, e.g.: Wu, IEEE-TAP, 1979; Resch, JPL TDA Progress Report, 1984; Gary et al., IEEE-TGRS, 1985; Robinson, Radio Science, 1988; Elgered, 1993; ...

R-series WVRs were developed at JPL in the late 70'ies– early 80'ies  
 Frequencies: 20.7 / 31.4 GHz  
 (Resch et al., JPL publ. 85-14, 1985)

Original design



Upgraded by NASA/GSFC  
 and Bendix with new positioner



Onsala WVR was developed 1978 – 1980  
 Frequencies: 21.0 / 31.4 GHz

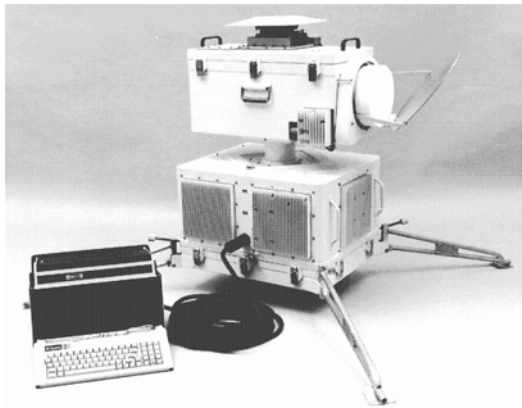
Original mounting in a fork (just like the R-series)

New mounting using mirror for elevation control from 1988



Used liquid nitrogen  
 load for calibration  
 during VLBI  
 experiments in the  
 80'ies, thereafter, only a  
 warm and a hot load.  
 Antenna beamwidths 6°

J-series WVR was developed in the mid 80'ies  
Frequencies: 20.7 / 22.2 / 31.4 GHz



Janssen, IEEE-TGRS 1985

## The ETH Water Vapour Radiometers

1st generation, here at Gothenburg-Landvetter Airport, 1992



2nd generation, on display at  
"Fundamentalstation Wettzell"

?

The Advanced Water Vapour Radiometer (AWVR) was developed especially for the high accuracy application for spacecraft tracking and search for gravitational waves (Tanner and Riley, Radio Science, 2003)



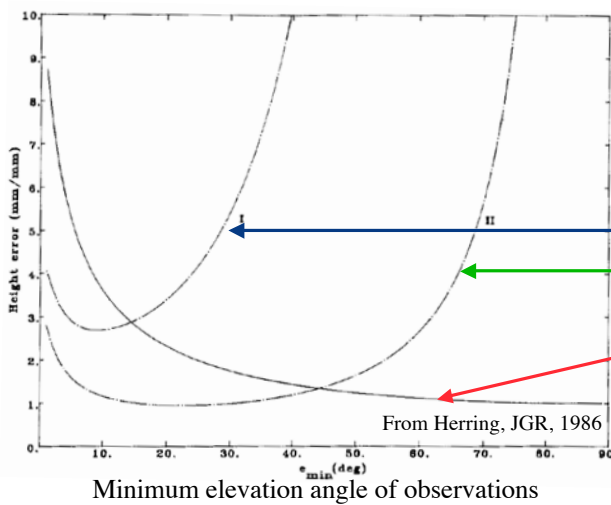
Frequencies:  
22.2, 23.8,  
31.4 GHz

Temperature stability of the electronics:  
 $35 \pm 0.005^\circ\text{C}$

From Oswald et al., IPN Progress Report, JPL, 2005

### To solve, or not to solve, for the atmosphere in VLBI

Propagation of zenith atmospheric errors into height errors



Random zenith variations when zenith delay parameters are,  
I: estimated  
II: not estimated

Bias error (if no estimation is carried out)

From Herring, JGR, 1986

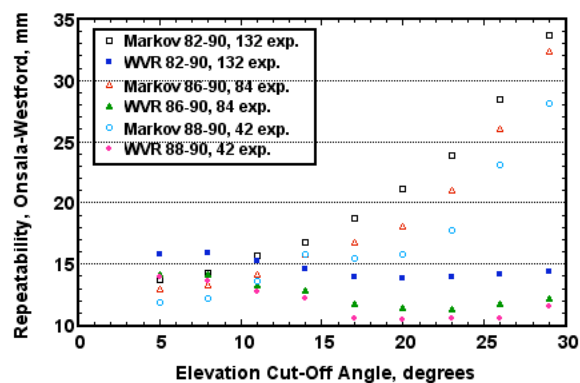
Minimum elevation angle of observations

## Studies using WVR data for wet delay corrections in VLBI

- Elgered et al., JGR, 1991
- Kuhn et al., Radio Science, 1991
- Elgered and Davis, European Working Meeting ..., Bad Neuenahr, 1993
- Emardson et al., J. of Geodesy,
- + an unknown number of case studies in Italy, South Africa, US, Germany ...

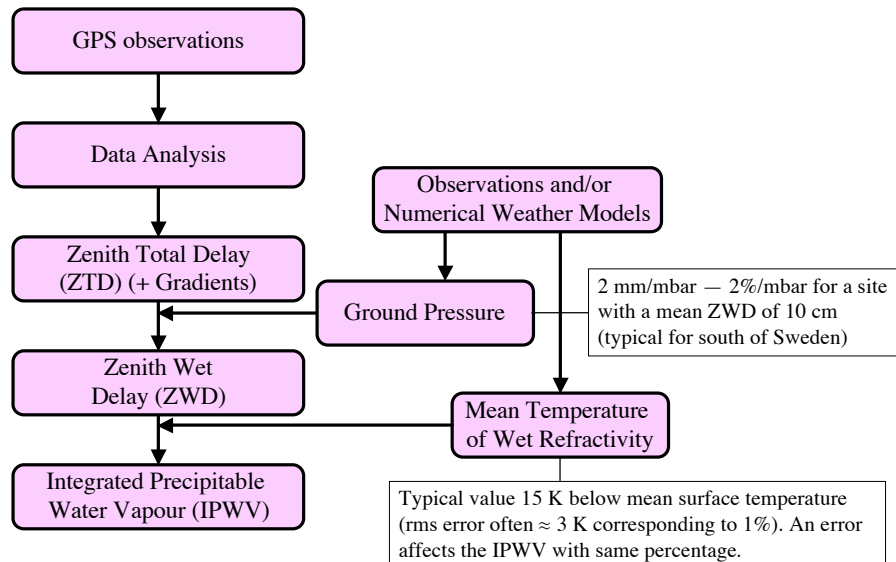
### Illustration of the WVR-in-VLBI problem

(note the improved quality of the VLBI data with time)

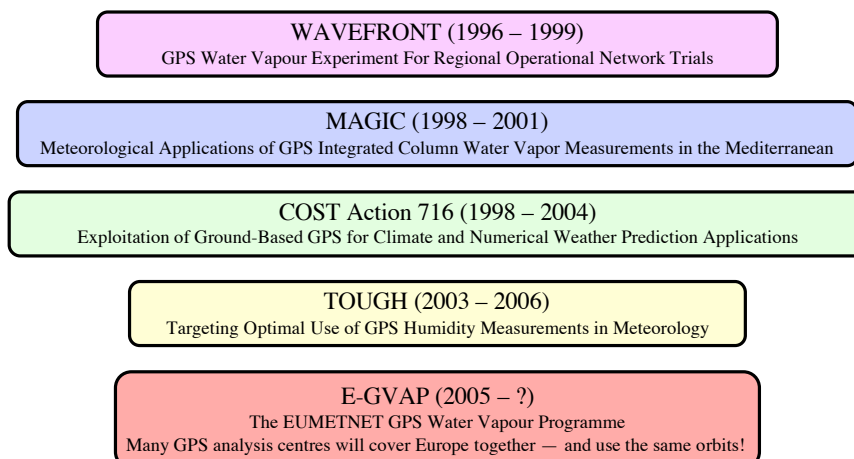


From Elgered and Davis (1993):  
Working Meeting in Bad Neuenahr

## Calculating water vapour time series from GPS data



## European research projects with the aim to use Ground-based GPS data in weather forecasting



### Spatial correlation of GPS estimation errors (Stoew et al., Final Report of the TOUGH project, 2005)

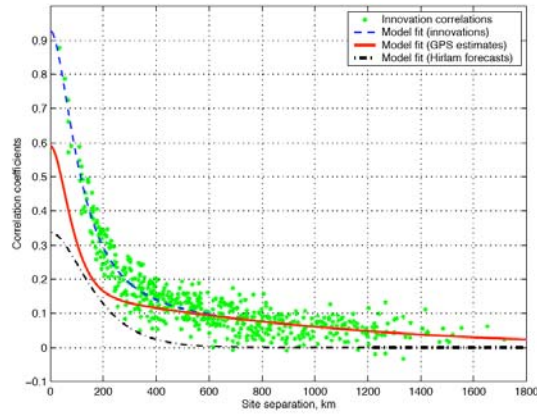
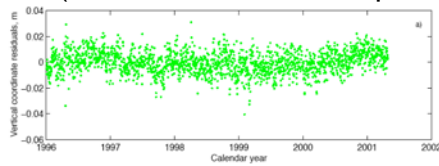
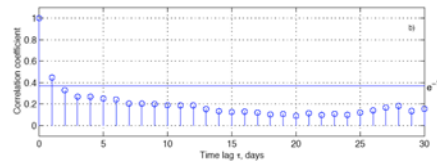


Fig. 6. Horizontal correlations of the ZTD innovations for a one year period (\*). The dash-dotted line represents the contribution of the forecast errors correlations for ZTD, estimated using the NMC method for HIRLAM at a resolution of 22 km. The dashed line shows the best-fit composite model for the innovation correlations. The solid line represents the remaining term, corresponding to the GPS error correlations.

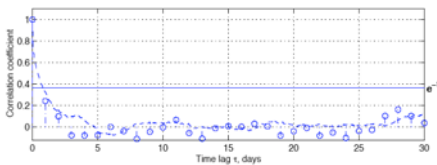
### Temporal correlation of GPS estimation errors (Stoew et al., Final Report of the TOUGH project, 2005)



GPS residuals of the  
Onsala vertical coordinate



Zenith wet delay  
differences (GPS – WVR)



## Sensitivity to climate change

What is the size of the trends in the water vapour content that we are searching for?

The increase of the global mean of IPWV is expected to be approximately 6 [%/K] (following the Clausius-Clapeyron relation assuming conservation of relative humidity [Trenberth et al., Bull. Am. Meteorol. Soc., 2003]).

ERA40 shows (Bengtsson et al. JGR, 2004):

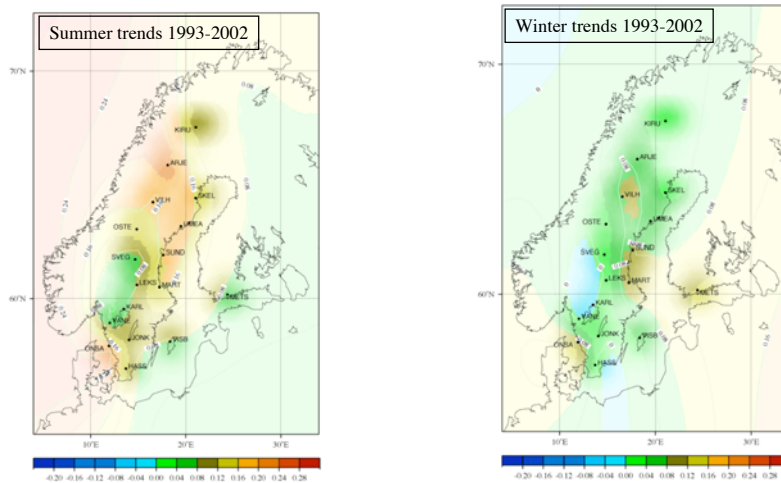
+0.11 K/decade in global temperature 1979–2001

+0.36 mm/decade in IPWV 1979–2001 — which is too large by a factor of 2 which is explained by artifacts in the global observing system.

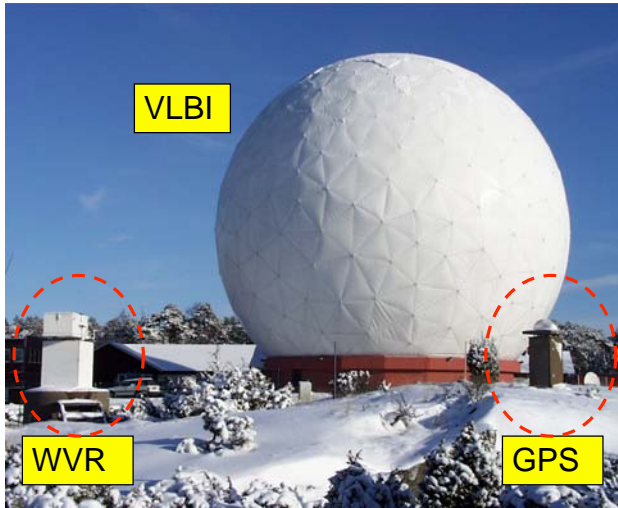
Trends of the order of 1 mm/decade could be expected at specific sites.

However, the annual averages at given sites shows much larger variability due to "weather".

Trends in the water vapour content for different seasons [mm/yr]  
(from Gradinarsky's PhD thesis 2002)



### Comparing water vapour trends from different techniques at the Onsala Space Observatory



+ Konrad WVR

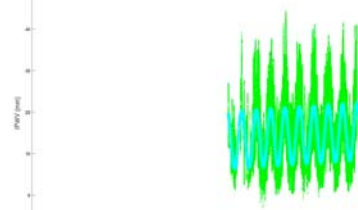
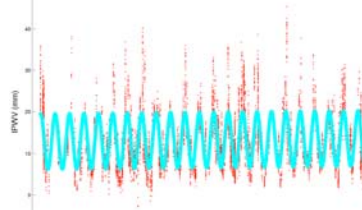


and radiosondes at about 38 km distance.

### Comparing trends from different techniques at Onsala

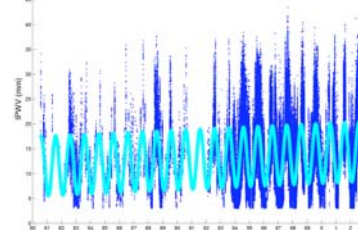
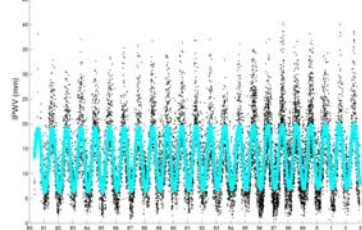
VLBI: Trend:  $+0.03 \pm 0.01$  mm/yr

GPS: Trend:  $+0.24 \pm 0.01$  mm/yr



RS: Trend:  $+0.04 \pm 0.01$  mm/yr

WVR: Trend:  $+0.13 \pm 0.01$  mm/yr



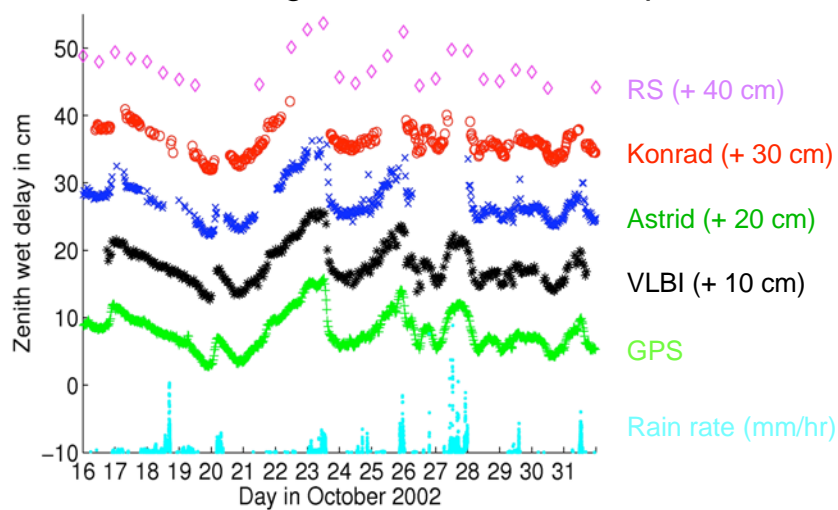
## Analysis of synchronized observations of the water vapour content at the Onsala Space Observatory:

	<i>rate diff. (mm/yr)</i>	<i>bias (mm)</i>	<i>rms (mm)</i>
V↔R	$0.02 \pm 0.02$	$+0.6 \pm 0.1$	2.1
V↔W	$0.06 \pm 0.02$	$+0.4 \pm 0.4$	1.6
V↔G	$0.02 \pm 0.03$	$-0.3 \pm 0.3$	1.3
G↔R	$0.06 \pm 0.02$	$+1.0 \pm 0.2$	2.0
G↔W	$0.00 \pm 0.02$	$+0.6 \pm 0.2$	1.5
W↔R	$0.01 \pm 0.03$	$+0.3 \pm 0.1$	1.7

V: VLBI (irregular 1980—2003)  
W: WVR (irregular 1980—2003)

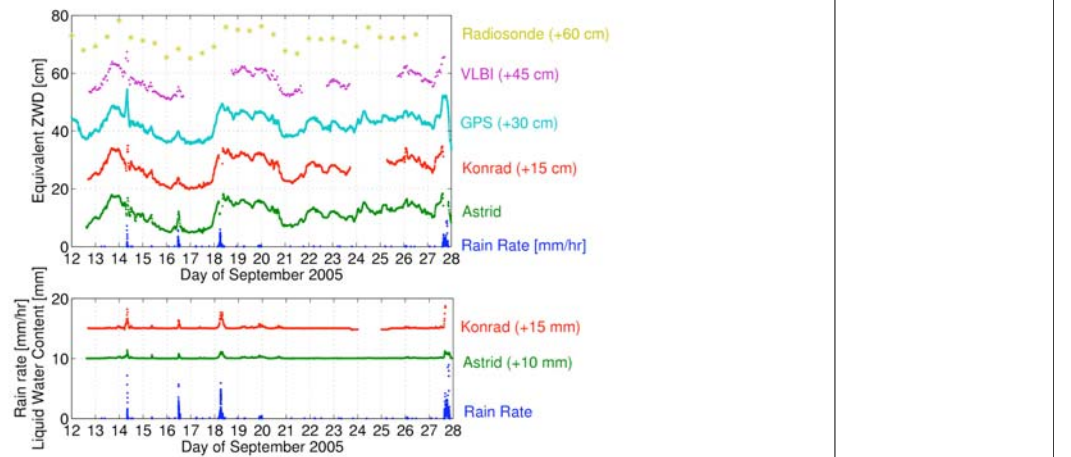
R: Radiosondes (1980—2003)  
G: GPS (1993—2003)

## Observations of the zenith wet delay and the rain rate at Onsala during the CONT2 VLBI experiment



## Zenith wet delay comparison: CONT05 VLBI experiment

Preliminary results from Rudiger Haas:



Using Astrid and Konrad WVRs to investigate atmospheric models (Nilsson et al., MicroRad meeting, Puerto Rico, 2006)

The equivalent zenith wet delay  $l_i$  in direction  $i$ :

$$l_i = \frac{10^{-6}}{m_i} \int_0^{\infty} N_w(\mathbf{x}_i(z)) dz$$

$m_i$ : mapping function,  $N_w$ : wet refractivity,  $\mathbf{x}_i(z)$ : position

The correlation between the refractivity at two locations is described by the equation:

$$\left\langle \left( N_w(\mathbf{x}_i) - N_w(\mathbf{x}_j) \right)^2 \right\rangle = 10^{-12} C_n^2 \left\| \mathbf{x}_i - \mathbf{x}_j \right\|^{2/3}$$

$C_n^2$ : refractivity structure constant

Using this equation we can calculate:

$$\left\langle \left( l_i - l_j \right)^2 \right\rangle$$

Unknown quantities:  $C_n^2$  and effective height of turbulence  $h$   
 The effect of both can be described by:

$$k^2 = \frac{C_n^2 h^{8/3}}{C_{n0}^2 h_0^{8/3}}$$

When using radiometer to test this model we have to take into account the instrumental noise:

$$\left\langle (l_i - l_j)^2 \right\rangle = k^2 \left\langle (l_i - l_j)^2 \right\rangle_0 + (m_i^{-2} + m_j^{-2}) \text{Var}[B] \quad (1 \text{ WVR})$$

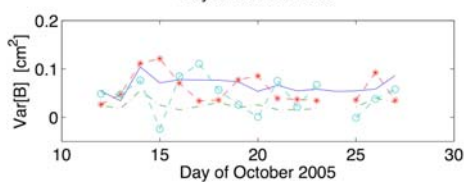
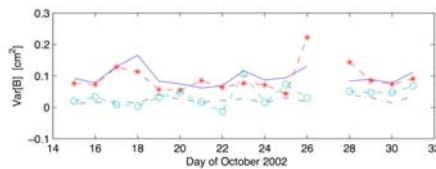
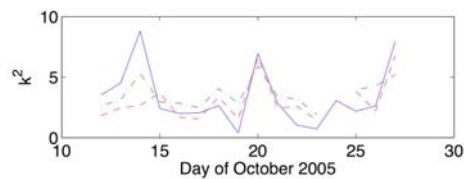
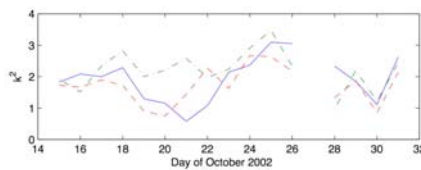
$$\left\langle (l_i - l_j)^2 \right\rangle = k^2 \left\langle (l_i - l_j)^2 \right\rangle_0 + m_i^{-2} \text{Var}[B_1] + m_j^{-2} \text{Var}[B_2] \quad (2 \text{ WVRs})$$

$\text{Var}[B]$ : variance of the instrumental noise

Results from:

CONT02

CONT05



Solid blue line: Astrid  
 Green dash-dotted line: Konrad

The short term noise of Astrid was reduced in 2003, which is confirmed by the lower variance during CONT05

## Conclusions: the role of microwave radiometry in support of space geodesy

- The VLBI 2010 plan does not include WVRs at all VLBI sites, but ...
- WVRs can provide independent data of high quality of the wet delay along the line of sight for:
  - assessment of estimates from space geodetic techniques
  - model development